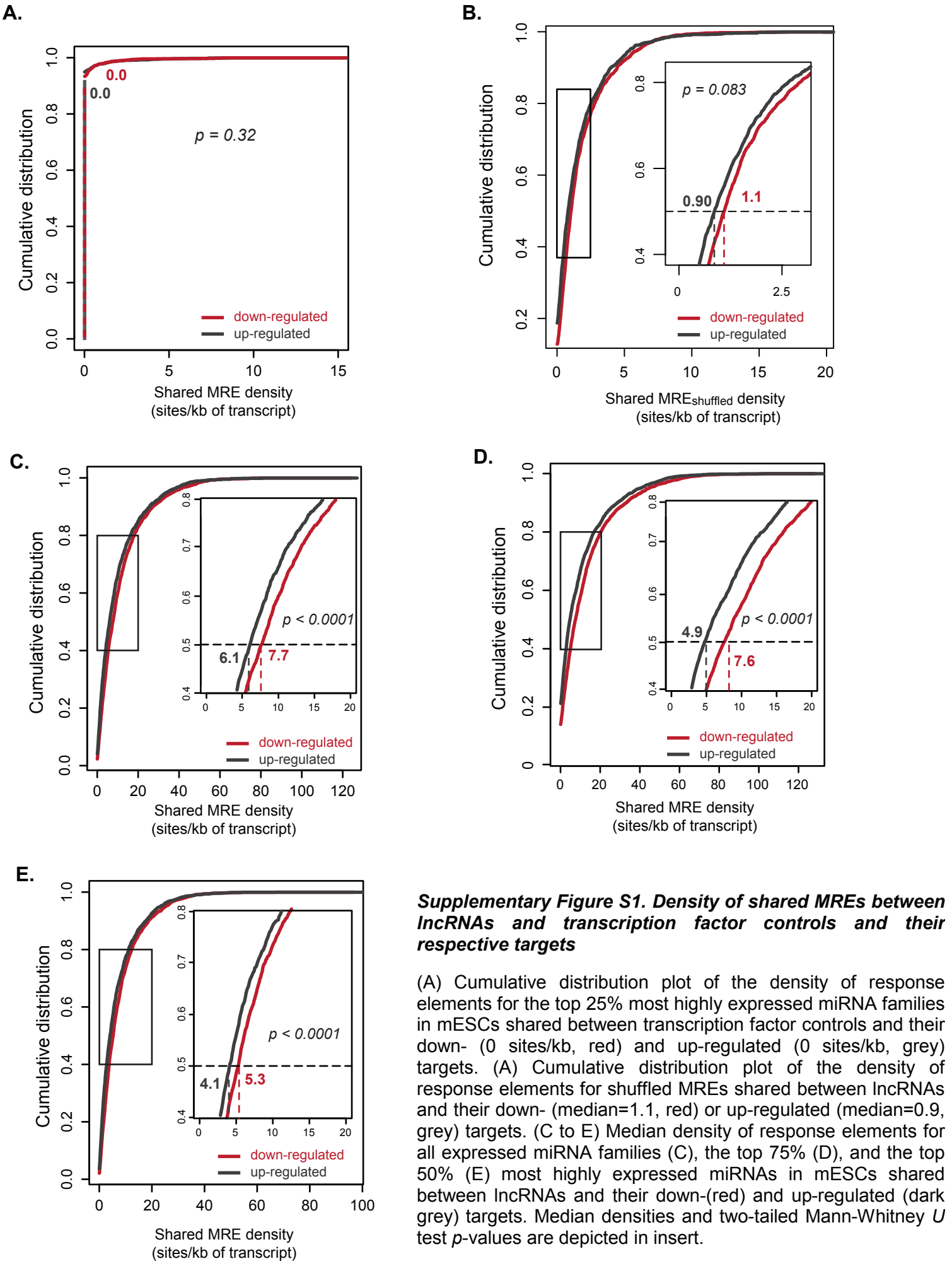


***Supplementary Figure S1. Density of shared MREs between lncRNAs and transcription factor controls and their respective targets***

(A) Cumulative distribution plot of the density of response elements for the top 25% most highly expressed miRNA families in mESCs shared between transcription factor controls and their down- (0 sites/kb, red) and up-regulated (0 sites/kb, grey) targets. (A) Cumulative distribution plot of the density of response elements for shuffled MREs shared between lncRNAs and their down- (median=1.1, red) or up-regulated (median=0.9, grey) targets. (C to E) Median density of response elements for all expressed miRNA families (C), the top 75% (D), and the top 50% (E) most highly expressed miRNAs in mESCs shared between lncRNAs and their down-(red) and up-regulated (dark grey) targets. Median densities and two-tailed Mann-Whitney *U* test *p*-values are depicted in insert.

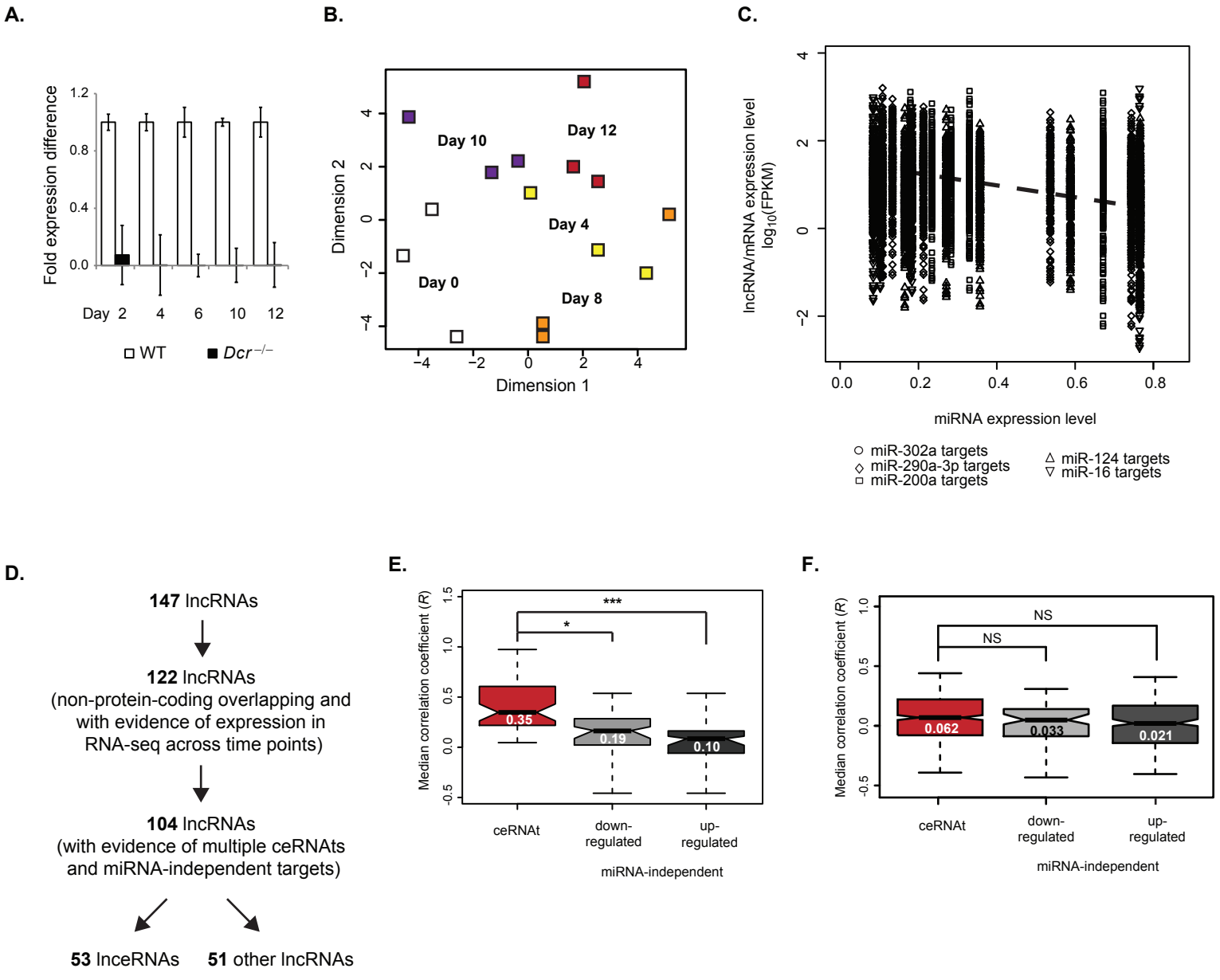


***Supplementary Figure S2. Gene expression patterns following loss of Dicer1 function.***

(A) Fold difference in *Dicer1 RNAseIII* domain expression ($Dcr^{-/-}$, black), relative to control (white) in mESCs following exposure to tamoxifen treatment, measured by qRT-PCR over a course of 12 days (X axis). (B) Multidimensional scaling (MDS) plot illustrating the separation of RNA sequencing data collected at each of the 5 time points (days 0-white, 4-yellow, 8-orange, 10-purple and 12-red) following Tamoxifen treatment in mESCs, each with 3 biological replicates. (C) Scatter plot representing the relationship between miR-302a (circle), miR-200a (square), miR-16 (inverted triangle), miR-290a-3p (diamond) and miR-124 (triangle) expression levels, measured by qPCR (Cross-threshold, CT, X-axis), with the expression of their respective mRNA and lncRNA targets, measured by RNA seq ($log_{10}$(FPKM), Y-axis), following the loss of *Dcr* function. Trend-line represented as dashed lines. (D) Flowchart illustrating filtering and classification of lncRNAs. (E) Distribution of the median correlation coefficients between the expression levels of lncRNAs and their respective ceRNAt (red, median $R$=0.35), down- (grey, $R$=0.19) and up-regulated (black, $R$=-0.10) miRNA-independent targets over the 12 day time course following the loss of miRNA biogenesis (*** $p$<0,001, two-tailed Mann-Whitney $U$ test). (F) Distribution of the median correlation coefficients between the expression levels of lncRNAs and their respective ceRNAt (red, median $R$=0.062), down- (grey, $R$=0.033) and up-regulated (black, $R$=-0.021) miRNA-independent targets for shuffled MREs over the 12 day time course following the loss of miRNA biogenesis (NS $p$>0.05, two-tailed Mann-Whitney $U$ test).

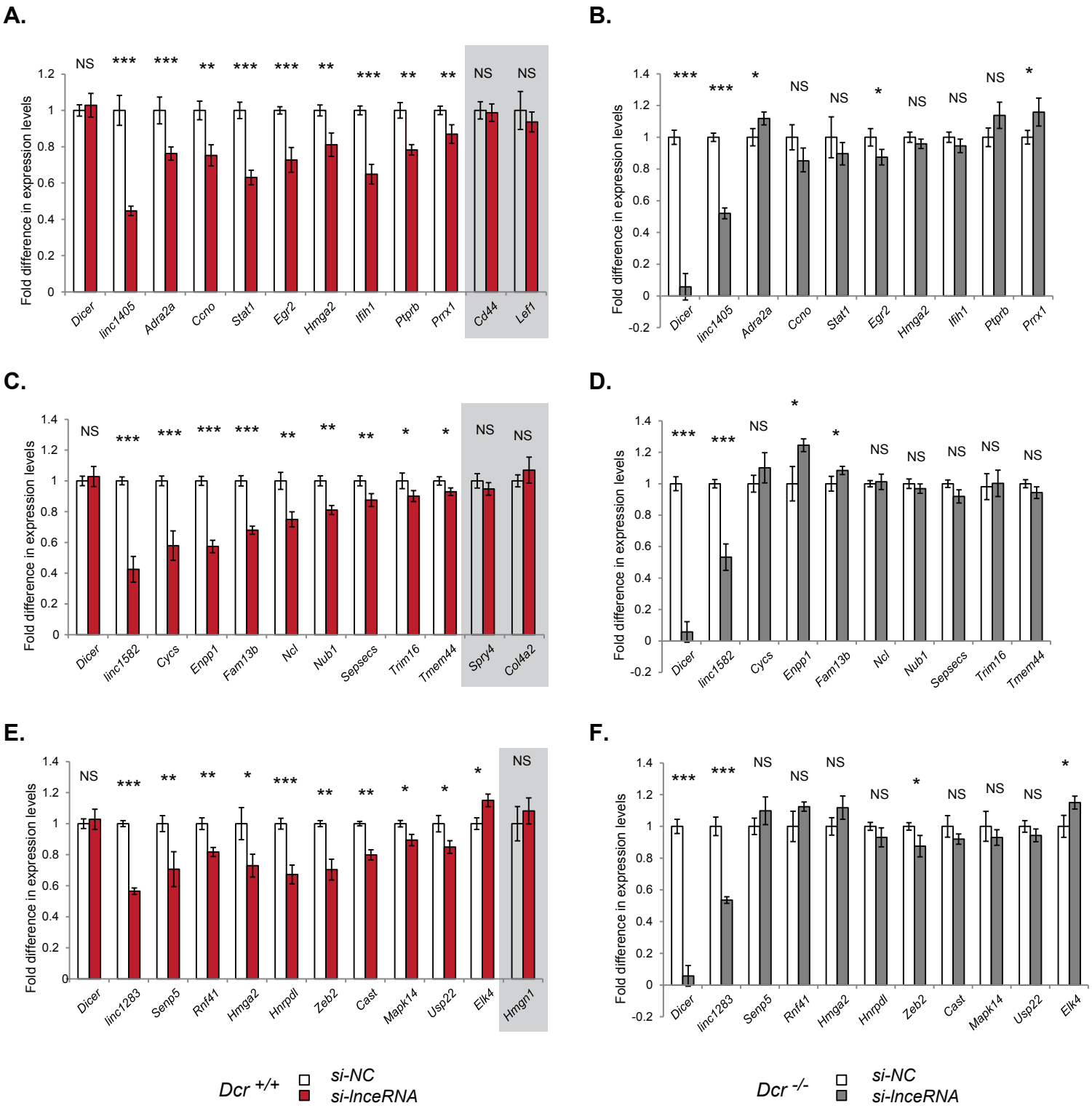


***Supplementary Figure S3. ceRNAt are down-regulated upon lnceRNA in Dcr$^{+/+}$ but not in Dcr$^{-/-}$ mESCs cells.***

(A) Fold difference in expression following knockdown of (A-B) *linc1405*, (C-D) *linc1582*, and (E-F) *linc1283*, using siRNAs in wild type (red, A, C and E) and *Dcr* null (grey, B, D and F) relative to siRNA transfection control (white). Putative ceRNAt whose expression levels were not affected by lnceRNA knockdown in *Dcr*$^{+/+}$ mESCs are highlighted by a grey shaded box and were not considered further.

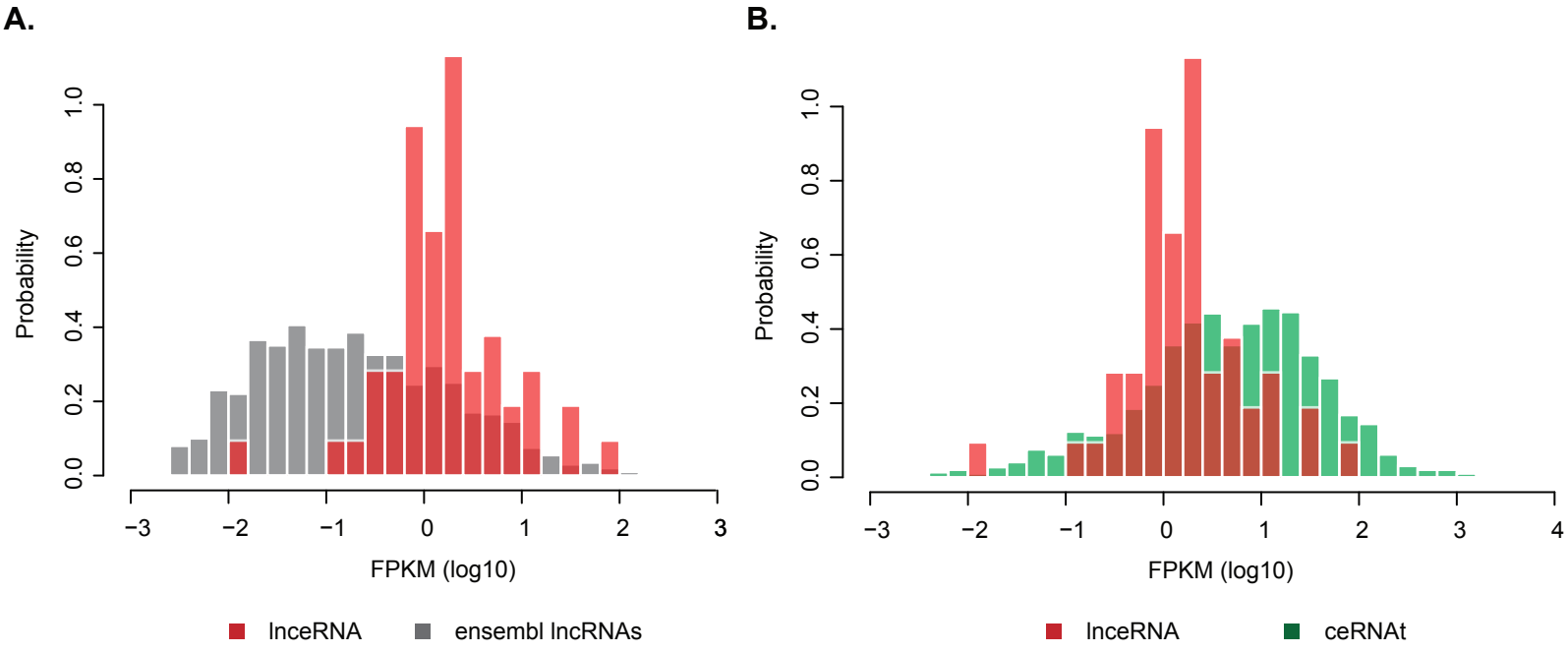


***Supplementary Figure S4. Relative lnceRNA expression.***

Cumulative distribution of the expression levels (measured by RNA-seq, log10(FPKM)) of (A) lnceRNAs (red) and Ensembl-annotated mESC-expressed lncRNAs (grey) and (B) lnceRNAs (red) and their ceRNAt (green).

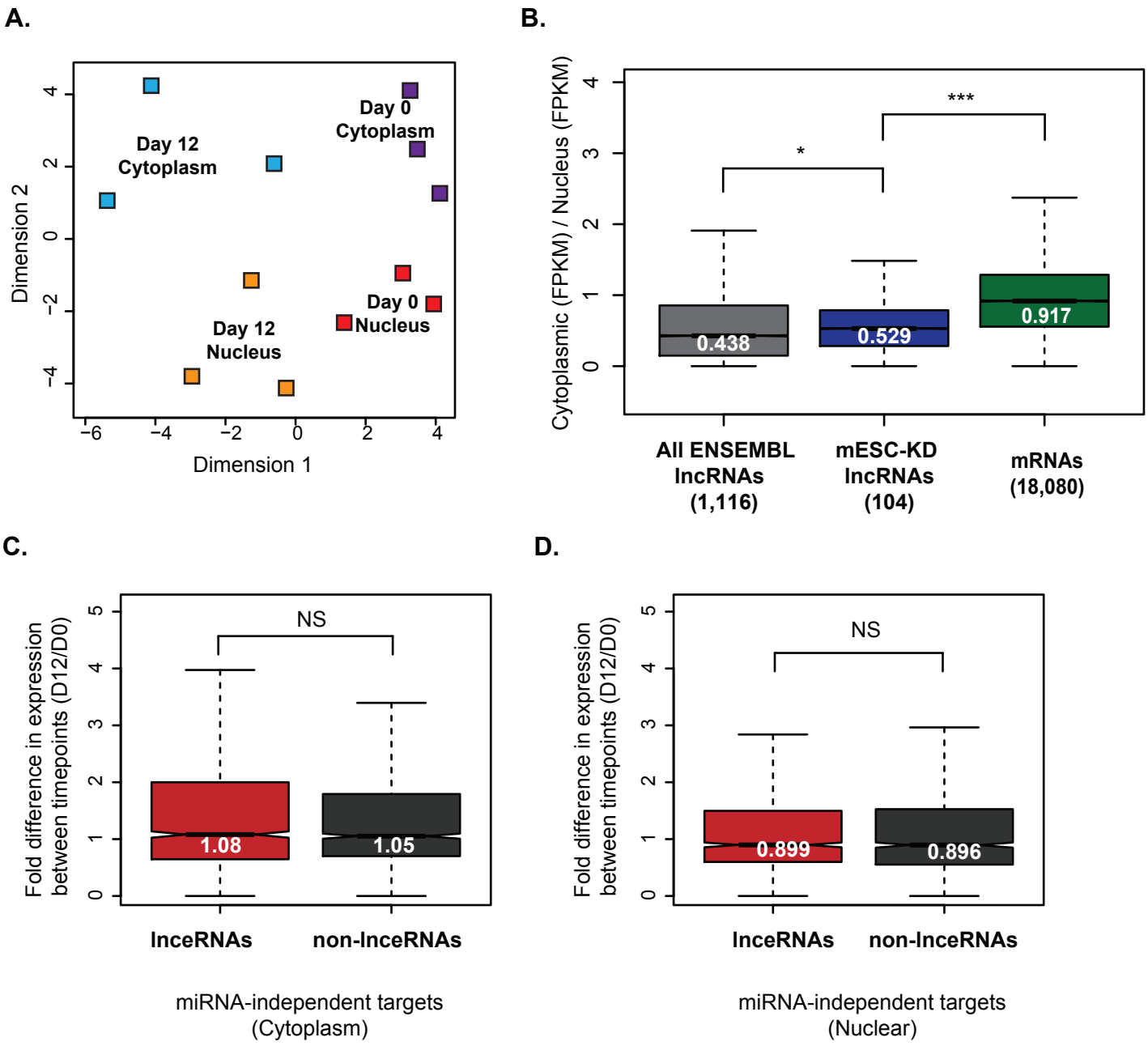


***Supplementary Figure S5. Gene expression patterns in the cytoplasm and nucleus of mESCs.***

(A) Multidimensional scaling (MDS) plot depicting RNA sequencing data of the cytoplasmic and nuclear subcellular fractions of mESCs before (day 0, cytoplasm-purple, nucleus-red) and 12 days after Tamoxifen treatment (cytoplasm-blue, nucleus-orange). (B) Distribution of the ratio between expression measured in the cytoplasm (FPKM) and nucleus (FPKM) for Ensembl (build 70) annotated lncRNAs (median $r$=0.438, dark grey), mESC-expressed lncRNAs (median $r$=0.529, blue) and Ensembl (build 70) mRNAs [(median $r$=0.917, green) (***, $p$<0.001 and * $p$<0.05]. (C and D) Distribution of the relative abundance of genes in the (C) cytoplasm and (D) nucleus of cells before (day 0) and after (day 12) *Dicer1* loss-of-function for miRNA-independent targets of the lnceRNAs (53) and those that not annotated as lnceRNAs (51 lncRNAs). NS, Not significant.

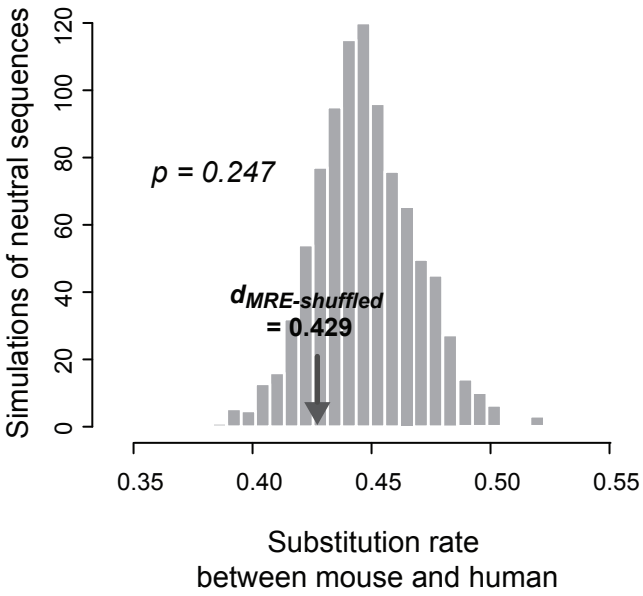


***Supplementary Figure S6. Sequence evolution of shuffled MREs in mammals.***

The substitution rate between, mouse and human, of shuffled MREs within lnceRNAs (vertical arrow, $d_{MRE\text{-}shuffled}$ = 0.429) is not significantly ($p$=0.247, empirical test) different relative to neutrally evolving sequence with the same length and with matching G+C content (ancestral repeats, ARs) in the vicinity of the lnceRNA (histogram).

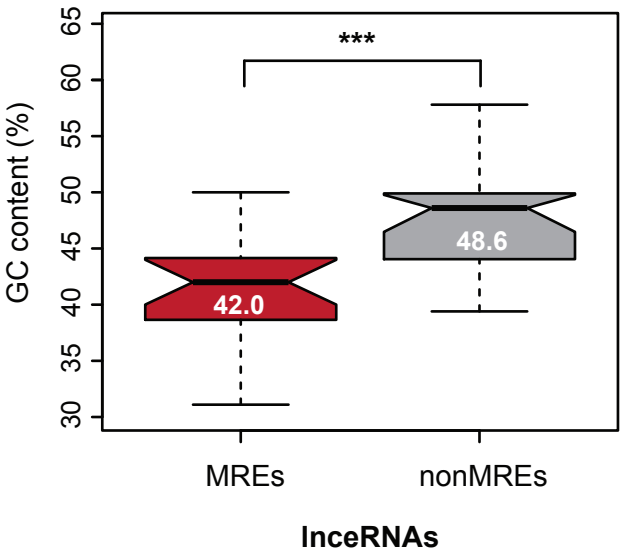


***Supplementary Figure S7. Sequence evolution of shuffled MREs in mammals.***

Distribution of G+C contents (X-axis) for MREs (median = 42.0%, red) and nonMREs (median = 48.6%, grey) sequence. ***, $p$<0.001.

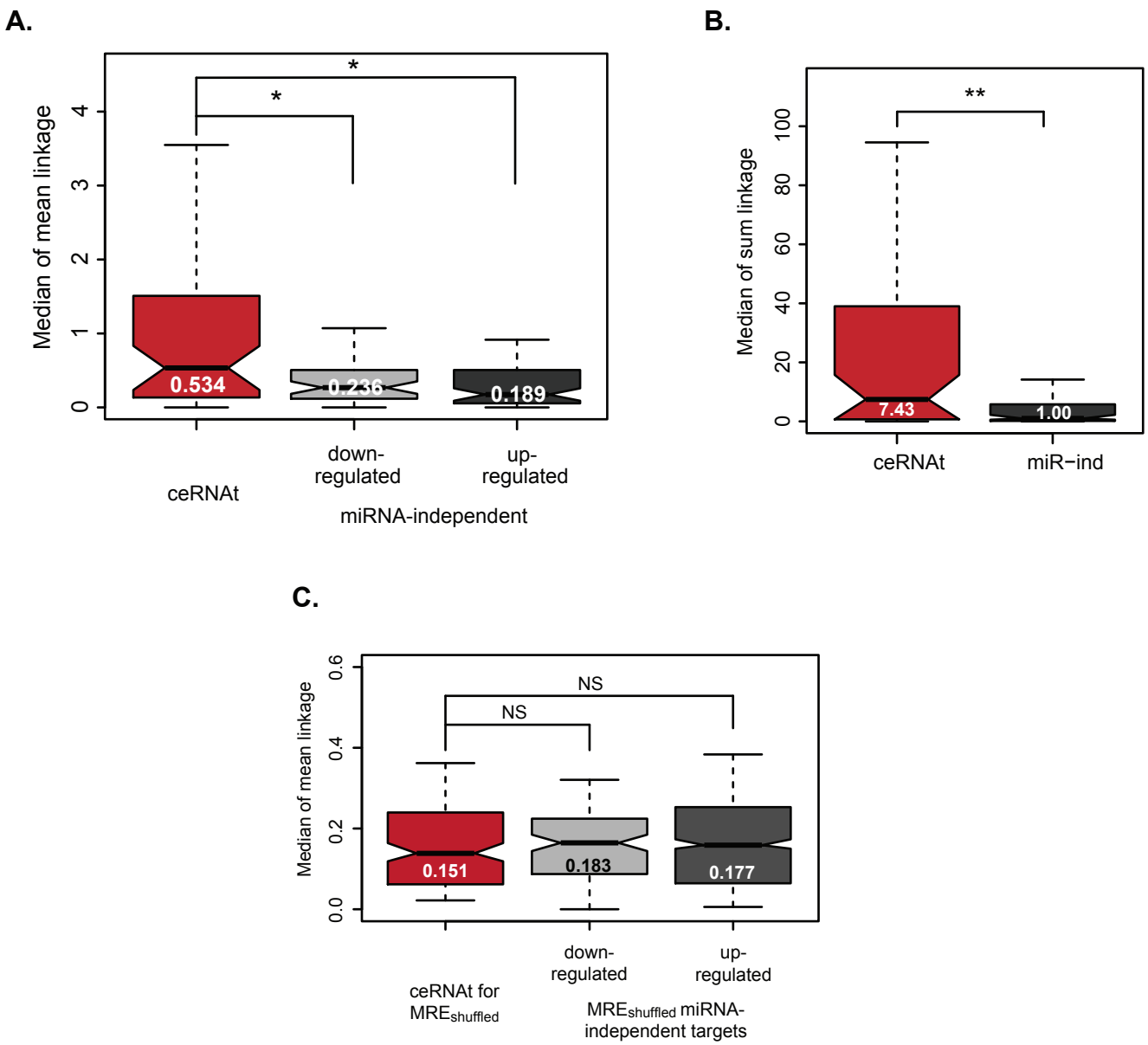


***Supplementary Figure S8. Functional relatedness of lnceRNA targets.***

(A) Distribution of the mean linkage in an integrative functional network (Honti et al. 2014), for ceRNAt (median of mean linkage=0.534, red) and their down- (median of mean linkage=0.236, light grey) and up-regulated (median of mean linkage=0.189, dark grey) miRNA-independent targets. (B) Distribution of the sum linkage for lnceRNA's ceRNAt (median of sum linkage=7.43, red) and miRNA-independent targets (median of mean linkage=1.00, dark grey) using an integrated functional network. (C) Distribution of the mean linkage in an integrative functional network (Honti et al. 2014), for ceRNAt (median of mean linkage=0.151, red) and their down- (median of mean linkage=0.183, light grey) and up-regulated (median of mean linkage=0.177, dark grey) miRNA-independent targets predicted using shuffled MREs. ***, $p<0.001$ ; *, $p<0.05$ and NS, not significant.

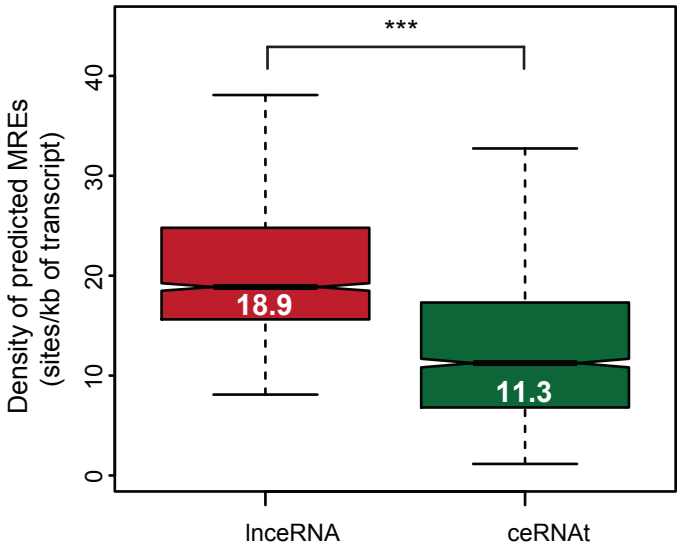


***Supplementary Figure S9. Distribution of MREs for lnceRNAs and protein-coding genes.***

Distribution of the density of predicted MREs for the top 25% most highly expressed miRNAs with lnceRNAs (median=18.9 MREs/kb, red) and their protein-coding gene 3'UTRs targets (green, median=11.3 MREs/kb). ***, $p<0.001$.

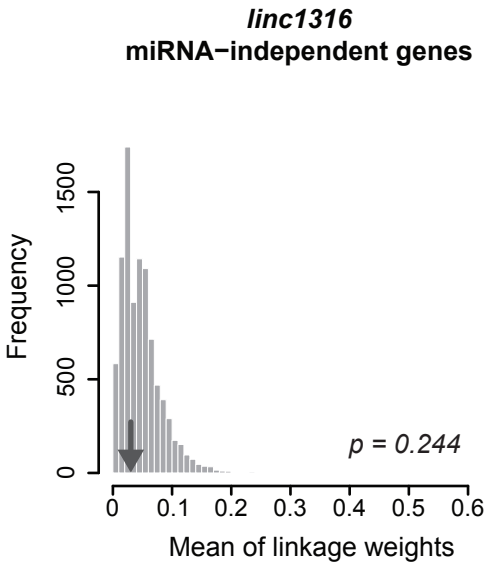


***Supplementary Figure S10. MicroRNA-independent targets of lnceRNA are not functionally related.***

MiRNA-independent targets of *linc1316* are not significantly (*p*=0.244, empirical *p* value) different in functional similarity than expected based on 10,000 sets with an equal number of randomly selected mESC-expressed genes.

## SUPPLEMENTARY TABLE LEGENDS

***Supplementary Table S1.*** Expression levels of mESC-expressed miRNAs. Unique miRNAs were grouped into miRNA families. Red shading highlights the 25% most highly expressed miRNAs.

***Supplementary Table S2.*** Number of ceRNAts and miRNA-independent target mRNAs per lncRNA predicted using the top 25% most highly expressed miRNAs.

***Supplementary Table S3.*** Classification of lncRNA's mRNA target as either competitive endogenous RNA targets (ceRNAt) or miRNA-independent targets (independent).

***Supplementary Table S4.*** lncRNAs overlapping protein-coding genes removed from the initial set of 147 lncRNAs.

***Supplementary Table S5.*** Pairwise correlation coefficient between lncRNAs and their ceRNAts and miRNA-independent targets.

***Supplementary Table S6.*** Relative expression levels in the cytoplasmic and nuclear subcellular fractions of mESC lncRNAs.

***Supplementary Table S7.*** Human conserved lnceRNAs.

***Supplementary Table S8.*** Density of MREs predicted within lncRNAs and protein-coding transcripts for the top 25% most highly expressed miRNAs in mESCs.

***Supplementary Table S9.*** Significantly enriched ceRNAt GO annotations.

***Supplementary Table S10.*** List of qRT-PCR primers used in the study.